Polymer Electrolytes Based on Acrylonitrile-Methyl Methacrylate-Styrene Terpolymers for Rechargeable Lithium-Polymer Batteries

Dong-Won Kim* **and Yang-Kook Sun***

Polymer Materials Laboratory, Samsung Advanced Institute of Technology, 103-12, Moonji-Dong, Yusung-Gu, Daejon 305-380, Korea

ABSTRACT

New polymer electrolytes composed of acrylonitrile-methyl methacrylate-styrene (AMS) terpolymer, 1 M $LiClO_4$-EC/PC, and an inorganic filler have been prepared. Depending on the composition of the components, these electrolytes exhibit a wide range of mechanical and electrical properties. The ionic conductivity reaches 1.4×10^{-3} S/cm in a polymer electrolyte containing 27% AMS terpolymer, 64% $LiClO_4$-EC/PC, and 9% silanized fumed silica at room temperature to give homogeneous films which exhibit good mechanical properties. These systems showed good compatibility with lithium electrodes and a sufficient electrochemical stability to allow safe operation in the rechargeable lithium batteries. The capacity and cycling performance of a Li/polymer electrolyte/$Li_{1.03}Mn_2O_4$ solid-state cell employing AMS-based polymer electrolyte were investigated.

Introduction

A large number of studies have been carried out on solid-state lithium batteries using gel polymer electrolytes in which the liquid electrolyte has been immobilized by incorporation into a matrix polymer, such as polyacrylonitrile (PAN),[1-3] poly (vinylidene fluoride) (PVdF),[4,5] and poly(vinyl chloride) (PVC).[6,7] These plasticized polymer electrolytes combine the best features of both liquid and solid electrolytes. Among these, PAN-based polymer electrolytes plasticized by liquid electrolyte solution showed the relatively high ionic conductivity of 10^{-3} S/cm at room temperature. However, these systems require processing at an elevated temperature at which PAN becomes soluble. Also poor compatibility with lithium electrodes and solvent exudation which might lead to cell leakage still remain crucial problems for their successful application in rechargeable lithium batteries.[2,8] One of the ways of solving these problems is the use of a copolymer as a matrix polymer. In our group, electrical properties of the plasticized polymer electrolytes based on acrylonitrile-methyl methacrylate copolymer or acrylonitrile-methyl methacrylate-(oligo oxyethylene) ethyl ether methacrylate terpolymer were investigated.[9,10] These studies demonstrated that the use of copolymers for polymer electrolytes allowed us to optimize physicochemical properties such as ionic conductivity, mechanical properties, compatibility with plasticizing electrolyte solution, and stability toward the lithium electrodes.

In this paper, we report the synthesis and some of the electrical properties of plasticized polymer electrolytes composed of acrylonitrile-methyl methacrylate-styrene terpolymer as a matrix polymer, plasticizing liquid electrolyte solution, and finely divided silica powder. The validity of using a newly developed polymer electrolyte for lithium batteries with a lithium anode and $Li_{1.03}Mn_2O_4$ composite cathode is also evaluated.

Experimental

Polymer synthesis.—High-purity acrylonitrile (AN), methyl methacrylate (MMA), and styrene (ST) were purchased from Aldrich and used without further purification. Poly(acrylonitrile-co-methyl methacrylate-co-styrene), P(AN-co-MMA-co-ST) was synthesized via emulsion polymerization with distilled water at 60°C in a glass reactor equipped with a nitrogen inlet, a reflux condenser, an additional funnel, and a mechanical stirrer. The molar ratio of co-monomers in the reaction feed was varied with a total monomer concentration of 1 mol/L. Potassium persulfate ($K_2S_2O_8$) was used as a free-radical water-soluble initiator, and sodium lauryl sulfate was used as an emulsifier. The polymerization was continued for 8 h with vigorous agitation. The polymer was isolated by filtration and washed successively with distilled water at 80°C to remove any impurities such as residual monomers and initiator. The product was then dried in a vacuum oven at 100°C for 24 h. A white powder was obtained as a final product. For brevity, the P(AN-co-MMA-co-ST) terpolymers synthesized are designated as AMS(x/y/z) in this paper, where x, y, z indicate the mole percent of AN, MMA, ST units in the terpolymer, respectively.

Characterization.—Proton nuclear magnetic resonance (^1H NMR) spectra were obtained in $CDCl_3$ or DMSO-d_6 solvent on a Bruker-DRX-400 NMR spectrometer with tetramethylsilane (TMS) as an internal standard reference. Gel permeation chromatography (GPC) was carried out using a Waters CV-150 instrument equipped with three μ-Styragel columns (10^3, 10^4, and 10^5 Å) and the system was calibrated with the monodisperse PS standards in THF. DSC thermal analysis was carried out to measure the glass transition temperatures with a heating rate of 10°C/min from −100 to 100°C.

Preparation of polymer electrolytes.—The AMS terpolymer was first dissolved in anhydrous THF. After the polymer was completely dissolved, a predetermined amount of liquid electrolyte, 1 M $LiClO_4$ in EC/PC (1:1 by volume, Mitsubishi Chemical Co., battery grade) was added and the solution was further stirred. The amount of electrolyte solution added was changed from 30 to 70 wt % based on the total weight of the polymer electrolyte composed of matrix polymer and liquid electrolyte. An appropriate amount of high purity silanized fumed silica (Cabot Co.) was then added, which had been treated with hexamethyldisilazane. When complete homogenization of the mixture was achieved, the resulting viscous solution was cast with a doctor-blade apparatus onto a release paper, then left to evaporate the solvent slowly at room temperature. After evaporation of THF, the film was separated from the release paper. The thickness of cast film was in the range of 60 ~ 200 μm. The polymer electrolyte was confirmed to be free of co-solvent by means of ^1H NMR. All procedures for preparing polymer electrolytes were carried out in a dry box filled with argon gas (99.999%).

Electrical measurements.—Polymer electrolyte film was cut into 4 cm^2 squares and sandwiched between two stainless steel (SS) electrodes. In order to investigate interfacial phenomena at the lithium electrode/polymer electrolyte interface, this sample was also sandwiched between two lithium electrodes (Cyprus Foote Mineral Co., 50 μm thick). An ac impedance measurement was then performed using a Zahner Elektrik IM6 impedance analyzer over the frequen-

---

* Electrochemical Society Active Member.

cy range of 0.1 Hz ~ 1 MHz with an amplitude of 10 mV. Each sample was allowed to equilibrate for 1 h at each temperature before measurement. A cyclic voltammetry experiment was carried out on a stainless steel working electrode with lithium electrodes as the counter and reference electrodes in the potential range of −1.0 to 4.5 V vs. Li at a scanning rate of 5 mV/s. The electrochemical stability window of the polymer electrolyte was measured by linear sweep voltammetry at a scanning rate of 1 mV/s.

$Li/Li_{1.03}Mn_2O_4$ cell.—A $Li_{1.03}Mn_2O_4$ composite cathode on an aluminum foil consisted of $Li_{1.03}Mn_2O_4$ with polymer electrolyte and super-P carbon in the proportions of 59:33:8 by weight percent. Spinel $Li_{1.03}Mn_2O_4$ was synthesized as described in the literature.[11] The anode consisted of 50 μm thick Li foil (Cyprus Foote Mineral Co.) and was pressed onto a Cu current collector. A rechargeable lithium-polymer cell was assembled by sandwiching the polymer electrolyte between the lithium anode and composite $Li_{1.03}Mn_2O_4$ cathode. The cell was then enclosed in a metallized plastic bag and vacuum sealed. All assemblies of the cell were carried out in a dry box filled with argon gas. Cycle tests of the lithium-polymer cell were conducted in the voltage range of 3.0 ~ 4.3 V at different current densities with galvanostatically controlled equipment.

Results and Discussion

The composition of the terpolymer was determined by a ^1H NMR spectrum, an example of which is shown in Fig. 1. In the ^1H NMR spectrum of the AMS terpolymer, the methine protons in the benzene ring of the ST unit appear separately at δ = 7.00 ~ 7.19 ppm, and the methoxy protons of the MMA unit are observed at δ = 3.33 ~ 3.59 ppm, whereas peaks of the methylene, methine, and methyl protons in the AN, MMA, and ST units observed at a higher field overlap one another. The relative intensities of the methylene and methine protons in the ST unit could be calculated by multiplying the intensity of the methine proton in the benzene ring by 3/5. The intensities of the methylene and methyl protons in MMA could be also estimated by multiplying the intensity of the methoxy protons which appeared at δ = 3.33 ~ 3.59 ppm by 5/3. The intensities of the methylene and methine protons in AN are determined by subtracting the calculated intensities of the methylene, methine, and methyl protons in ST and MMA from the total intensities of peaks superimposed at δ = 0.83 ~ 2.93 ppm. The mole fraction of each co-monomer unit can thus be estimated by the total intensity of the corresponding monomer unit. The molar composition of AN, MMA, and ST was determined to be 57:27:16 from the ^1H NMR spectrum shown in Fig. 1. The molar compositions of the terpolymers we synthesized are summarized in Table I.

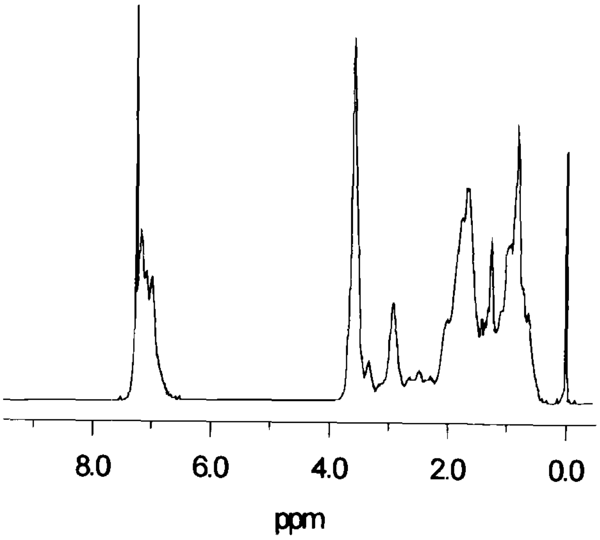

Fig. 1. ^1H NMR spectrum of AMS terpolymer in $CDCl_3$ at 25°C.

Table I. Molar compositions, average molecular weights, and glass transition temperatures of AMS terpolymers.

Polymer	Molar composition (AN:MMA:ST)	Molecular weight M_n	Molecular weight M_w	T_g (°C)
AMS (12/54/34)	12:54:34	1,346,000	2,924,000	105.0
AMS (16/42/42)	17:42:42	1,289,000	2,887,000	103.6
AMS (32/31/37)	32:31:37	1,179,000	2,454,000	102.1
AMS (47/31/22)	47:31:22	2,021,000	3,416,000	103.8
AMS (52/43/5)	52:43:5	2,187,000	4,046,000	101.2
AMS (57/27/16)	57:27:16	2,400,000	4,055,000	108.1

The average molecular weights and glass transition temperatures of AMS terpolymers are also given in Table I. Only one glass transition for each AMS was observed in the temperature range of 102 to 108°C, which is a typical behavior of the glass transition observed in a random copolymer. It is also found that the T_g value is little dependent on the molar composition of terpolymers, which may be caused by the small difference in glass transition temperatures among the component polymers. Glass transition temperatures of PAN, PMMA, and PS homopolymers were measured to be 97, 110, and 100°C, respectively. The molecular weights are very high, and the polydispersity indexes range from 1.7 to 2.2.

Figure 2 shows a typical ac impedance spectrum of the SS/solid polymer electrolyte at room temperature. The polymer electrolyte consisted of 30% AMS (47/31/22) terpolymer and 70% $LiClO_4$-EC/PC by wight. The plot consists of a spike displaced from the orgin, which represents a resistor in series with a capacitor. This result suggests that the resistive component of the polymer electrolyte is dominant. Ions can be transported quickly in the liquid phase as the electric potential alternates between positive and negative in an ac field. Therefore no capacitance effects were observed in the polymer electrolytes. The intercept on the real axis gives the electrolyte resistance. The ionic conductivity was estimated to be 1.0×10^{-3} S/cm from the bulk resistance found in this figure.

Figure 3 shows the ionic conductivities of polymer electrolytes prepared with the AMS terpolymers listed in Table I, as a function of liquid electrolyte content. The ionic conductivity increases with the amount of electrolyte solution in the polymer electrolyte. The improved ionic conductivity is due to the enhancement of the ionic mobility and number of carrier ions, as reported.[12] When the amount of electrolyte solution exceeds about 50%, the

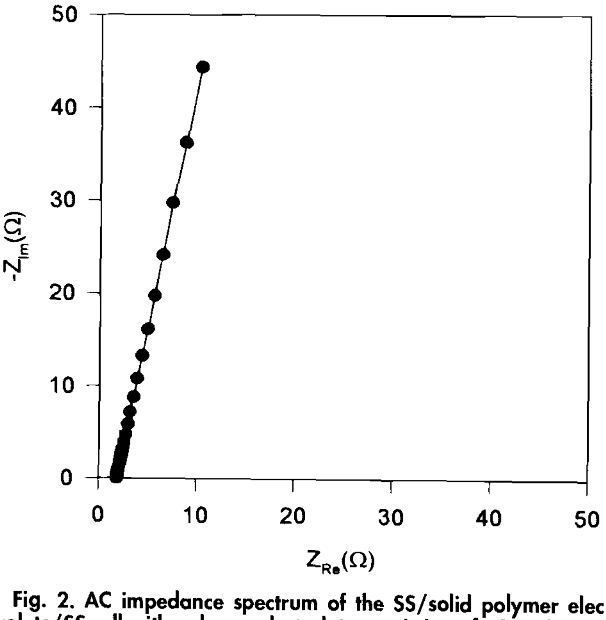

Fig. 2. AC impedance spectrum of the SS/solid polymer electrolyte/SS cell with polymer electrolyte consisting of 30 wt % AMS (47/31/22) and 70 wt % $LiClO_4$-EC/PC at 25°C.

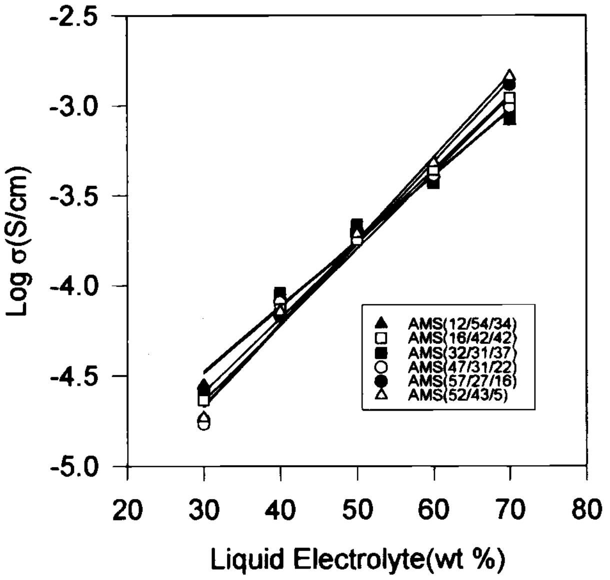

Fig. 3. Ionic conductivities of AMS-based polymer electrolytes as a function of liquid electrolyte content at 25°C.

ionic conductivity appeared to decrease with the content of ST in AMS terpolymers. This result may be due to the fact that liquid electrolyte in the polymer matrix exuded due to the poor compatibility between the ST unit in the terpolymer and aprotic solvents such as EC and PC. The mechanical state of these polymer electrolytes was found to be dependent on molar composition in the AMS terpolymer. With increasing MMA content in the terpolymer, the addition of electrolyte solution rendered the polymer electrolyte more flexible. For example, a polymer electrolyte prepared with AMS (52/43/5) containing 70 wt % of liquid solution was sticky and difficult to handle. From these results, it can be said that the relative AN/MMA/ST molar ratio in the terpolymer plays an important role in determining the ionic conductivity, the capacity to retain electrolyte solution and the mechanical strength of the cast film. In further experiments, the AN/MMA/ST molar composition will be restricted to 57/27/16. With 70 wt % of liquid electrolyte solution, the polymer electrolytes prepared with AMS (57/27/16) exhibited an ionic conductivity of 1.3×10^{-3} S/cm.

It is known that the addition of inert filler is a useful tool for increasing the electrical and mechanical properties of polymer electrolytes.[13,14] In order to enhance the physical strength of the polymer electrolyte film, silanized fumed silica was added to a polymer electrolyte containing 30% AMS terpolymer and 70% $LiClO_4$-EC/PC. Silica is very fine dry powder with a Brunauer-Emmett-Teller (BET) surface area of 212 m^2/g. The influence of the silica powder content on the ionic conductivity is shown in Fig. 4. It is found that the ionic conductivity reaches a maximum at 5 wt % of silica. An increase of conductivity with the addition of silica up to 5 wt % is related to the enhancement of capacity to hold liquid electrolyte, since it has a high adsorption capability, and subsequently enables loading of the plasticizing solvent. In addition, the presence of finely divided inorganic fillers is shown to reinforce the physical strength of the film, such as tear strength. This reinforcement is related to the fact that the fine ceramic powder is homogeneously dispersed into a liquid electrolyte and forms a three-dimensional network which mechanically supports the solution. On the other hand, further addition of the silanized fumed silica had little effect on the absorbancy of liquid electrolyte. With more than 5 wt % silica in the composite polymer electrolyte, the addition of silica powder decreases ionic conductivity due to the restriction of ionic motion. For the systems under study, the optimum filler content is believed to be 5 ~ 10% in terms of both ionic conductivity and mechanical stability.

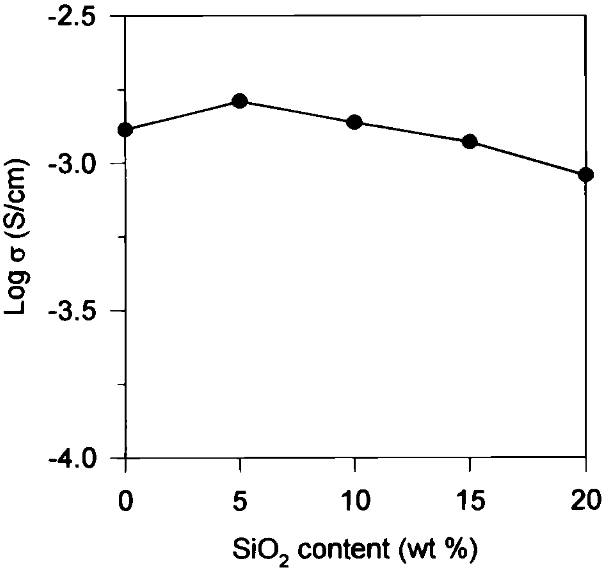

Fig. 4. Ionic conductivities with SiO_2 content for AMS (57/27/16)-based polymer electrolytes containing 70 wt % liquid electrolyte at 25°C.

Figure 5 shows the Arrhenius plot of ionic conductivities for polymer electrolytes containing 27% AMS (57/27/16), 64% liquid electrolyte, and 9% silica by weight, respectively. For this system, the ionic conductivity reaches the order of 1.4×10^{-3} S/cm at room temperature, and the conductivity remains high (1.7×10^{-7} S/cm) even at −20°C. It has been reported that an abrupt decrease in ionic conductivity observed at low temperatures in the plasticized polymer electrolyte is related to the crystallization of plasticizing solvent.[3] Because the MMA unit in the AMS terpolymer has a carbonyl group (-COO-) in the side chain, strong specific interaction between the MMA unit, and aprotic solvent makes the plasticizer difficult to phase-separate from a matrix polymer. This behavior could lead to the retardation of crystallization of the aprotic solvent, which results in the absence of an abrupt decrease in ionic conductivity at low temperatures.

The compatibility of an electrolyte with the lithium electrode is essential to guarantee acceptable performance and

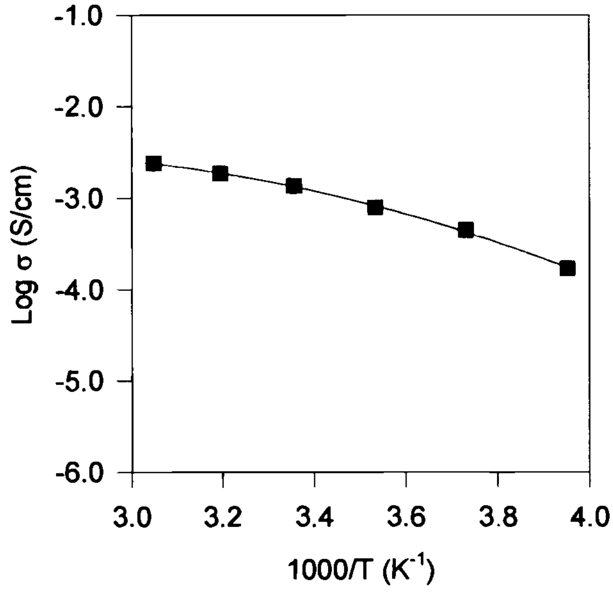

Fig. 5. Temperature dependence of ionic conductivity for a polymer electrolyte containing 27% AMS (57/27/16), 64 wt % liquid electrolyte and 9% silica.

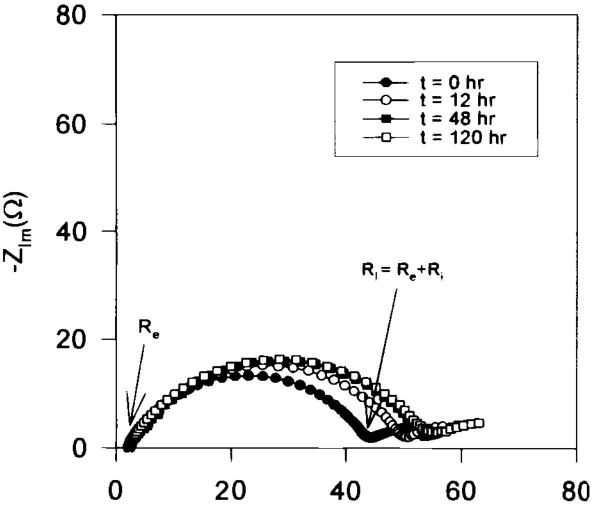

Fig. 6. AC impedance spectra of a Li/solid polymer electrolyte/Li cell as a function of storage time at 25°C, where the solid polymer electrolyte consists of AMS (27 wt %), 1 M $LiClO_4$ in EC/PC (64 wt %) and SiO_2 (9 wt %).

lifetime in rechargeable lithium-polymer batteries, and we therefore tried to investigate the interfacial behavior of a lithium electrode in contact with the polymer electrolyte under prolonged exposure. Figure 6 shows the time evolution of the ac complex impedance response of a Li/polymer electrolyte/Li cell under open-circuit potential conditions at 25°C. From these impedance spectra, it is possible to represent the time evolution of electrolyte resistance (R_e) and interfacial resistance (R_i), as shown in Fig. 7. The electrolyte resistance is the intercept on the real axis at high frequency, and the interfacial resistance is calculated from the difference between the intercept (R_l) at low frequency and R_e. It is found that the resistance of the polymer electrolyte maintains a constant value, independent of time. This result suggests that the encapsulated liquid electrolyte in the polymer matrix was not lost in the closed Li/solid polymer electrolyte/Li cell. The interfacial resistance increased initially, and eventually stabilized at a constant value of about 51 Ω (204 Ω cm^2). The initial increase can be attributed to the formation of a passive layer due to the reactivity of the lithium electrode and the polymer electrolyte. Given the intrinsic stability of the polymer backbone, one might speculate that the lithium electrode reacts with carbonated-based electrolytes. Aprotic solvents such as EC and PC are well known for forming a passivating layer on lithium metal.[15-17] On the contrary, the final steady-state value of R_i suggests the absence of further growth of the passive film. This result can be attributed to the immobilization of aprotic solvent in the polymer electrolytes. The aprotic solvents are well encapsulated in the matrix polymer due to the good compatibility between terpolymer and solvent, which reduces the reactivity of aprotic solvent towards lithium metal. Moreover, the organic solvent can be immobilized within the three-dimensional network of fumed silica. An apparent increase in stability of the lithium passive film in the presence of fumed silica is congruent with results reported by Fan and Fedkiw.[14]

The cyclic voltammogram for the Li/polymer electrolyte/SS cell at room temperature is given in Fig. 8. On sweeping the electrode cathodically, a cathodic peak is observed at about −0.54 V, which corresponds to the plating of lithium onto the stainless steel electrode. On the reverse scan, stripping of lithium is observed at about 0.41 V. The voltammograms ascribed to lithium deposition/dissolution are highly reversible, because the integrated charges in the cathodic and anodic processes are equal. The peak current tends to decrease slightly with cycling and stabilizes after a few cycles. On further sweeping the electrode to 4.5 V, there appear no additional oxidation peaks related to the decomposition of polymer electrolyte. From the linear sweep voltammetry experiments, this polymer electrolyte system was proved to be electrochemically stable up to 4.6 V vs. Li.

To demonstrate the usefulness of the AMS-based polymer electrolyte in rechargeable lithium batteries, we fabricated a Li/solid polymer electrolyte/$Li_{1.03}Mn_2O_4$ cell using the polymer electrolyte and $Li_{1.03}Mn_2O_4$ composite cathode. In order to reduce capacity fading and improve cyclability of $LiMn_2O_4$ powders in the 4 V region, the excess lithium (0.03) to the stoichiometric $LiMn_2O_4$ is added in preparation of spinel $Li_{1.03}Mn_2O_4$ powder. The $Li_{1.03}Mn_2O_4$ powders have shown good discharge capacity and excellent cyclability.[11] Figure 9 shows the charge-discharge curves with number of cycles for Li/solid polymer electrolyte/ $Li_{1.03}Mn_2O_4$ cell at a constant current density of 0.1 mA/cm^2. The spinel $Li_{1.03}Mn_2O_4$ is well known to be a high-voltage cathode

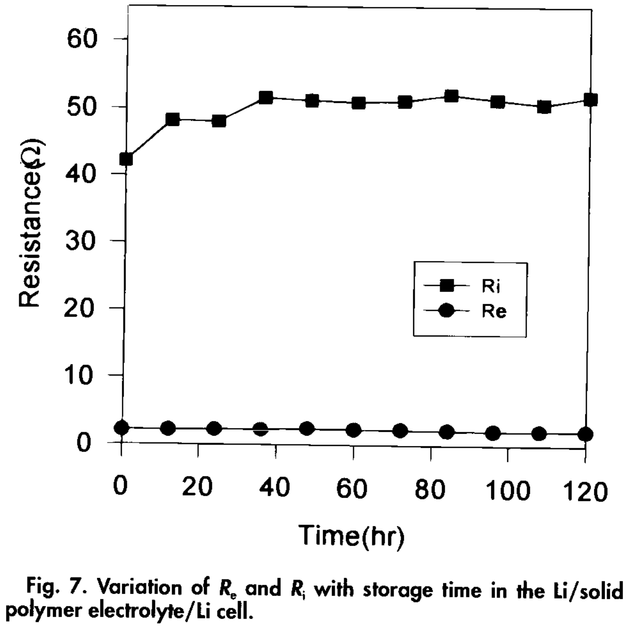

Fig. 7. Variation of R_e and R_i with storage time in the Li/solid polymer electrolyte/Li cell.

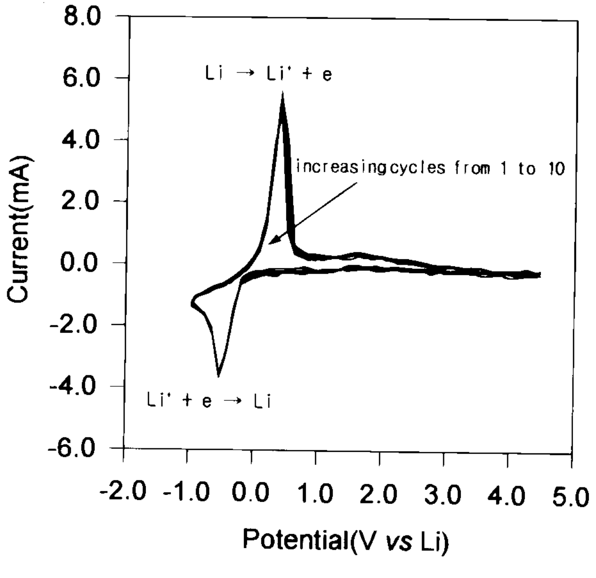

Fig. 8. Cyclic voltammogram of the Li/solid polymer electrolyte/SS cell at 25°C (scan rate: 5mV/s), where the solid polymer electrolyte consists of AMS (27 wt %), 1 M $LiClO_4$ in EC/PC (64 wt %) and SiO_2 (9 wt %).

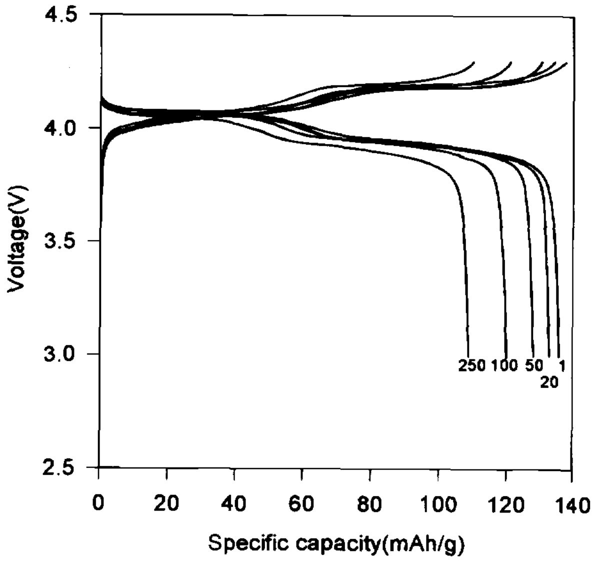

Fig. 9. Cycling curves for Li/solid polymer electrolyte/ $Li_{1.03}Mn_2O_4$ cell with repeated charge/discharge cycles at 0.1 mA/cm^2 (0.2 C rate).

which releases lithium ions according to the following cell process

$$Li_{1.03}Mn_2O_4 \underset{\text{discharge}}{\overset{\text{charge}}{\rightleftharpoons}} Li_{1.03-x}Mn_2O_4 + xLi$$

This figure shows that the charge-discharge curves have two distant plateaus, which is characteristic of the manganese oxide spinel structure.[18,19] It has been reported that each plateau delivered half of the total capacity, which confirmed the hypothesis that there were two binary equilibrium states during Li^+ intercalation.[18] These are λ-MnO_2-$Li_{0.5}Mn_2O_4$ and $Li_{0.5}Mn_2O_4$-$LiMn_2O_4$, respectively. The coulombic efficiency of this cell was about 100%. The Li/solid polymer electrolyte/$Li_{1.03}Mn_2O_4$ cell initially delivered 135 mAh/g based on $Li_{1.03}Mn_2O_4$ active material. Figure 10 shows the discharge capacities as a function of cycle number in the Li/solid polymer electrolyte/ $Li_{1.03}Mn_2O_4$. The discharge capacity reached a maximum value on the seventh cycle, and then slowly decreased with further cycling. An initial increase of discharge capacity up to seventh cycle may be due to the fact that the interfacial properties are improved during initial charge-discharge cycles of the cell. The discharge capacity remained at about 109 mAh/g at the 250th cycle, which was 80% of initial capacity. The capacity decline of the Li/solid polymer electrolyte/$Li_{1.03}Mn_2O_4$ cell may be related to the deterioration of interfacial contacts ($Li_{1.03}Mn_2O_4$/conducting carbon/polymer electrolyte) for the composite cathode as a result of lattice changes of the cathode active material during charge-discharge cycling. A significant strain on the interface of the composite cathode is believed to degrade the electrical contact between the surfaces of the insertion particles, and hence to decrease the capacity of the cathode during repeated charge-discharge cycling.

The ac impedance technique could provide useful information on the charge transfer and diffusion of lithium ions in the $Li_{1.03}Mn_2O_4$ electrodes. Figure 11 shows the ac impedance spectra of a Li/solid polymer electrolyte/ $Li_{1.03}Mn_2O_4$ cell with repeated cycling. The diagrams reveal that the low-frequency semicircle expands with repeated cycling and this in turn indicates an increase of the interfacial resistance of the composite cathode. This may be caused by continual volume change in the composite cathode. A similar result has been also reported on a composite V_6O_{13} cathode.[20] The ac impedance diagram is completed by a Warburg line related to the diffusion of the Li^+ within $Li_{1.03}Mn_2O_4$, which is qualitatively similar to those obtained in liquid organic electrolytes.[21] This indicates that the kinetics of the electrochemical intercalation process may become diffusion controlled.

Figure 12 represents the charge/discharge curves of the Li/solid polymer electrolyte/$Li_{1.03}Mn_2O_4$ cell obtained at different charge-discharge rates. The cell delivered a capacity of 136 mAh/g at a 0.125 C rate. It also showed the attractive capacity of 121 mAh/g at the 0.7 C rate. However, it is found that the polarization was increased as the current rate increased, which results in a decrease of capacity. The discharge capacity is found to drop to 68 mAh/g at the 1.25 C rate. With the same $Li_{1.03}Mn_2O_4$ spinel cathode material, a discharge capacity of 128 mAh/g at the 1.7 C rate has been reported in a Li/1 M $LiBF_4$, EC-DEC/$Li_{1.03}Mn_2O_4$ cell.[11] Thus, the reduced capacity in the Li/polymer electrolyte/ $Li_{1.03}Mn_2O_4$ cell at high rates can be related to the lower diffusion rate of lithium ions in the polymer electrolyte as compared to that of liquid electrolyte solution. More detailed studies are in progress for obtaining definite clarification of diffusion kinetics in composite electrodes and polymer electrolytes.

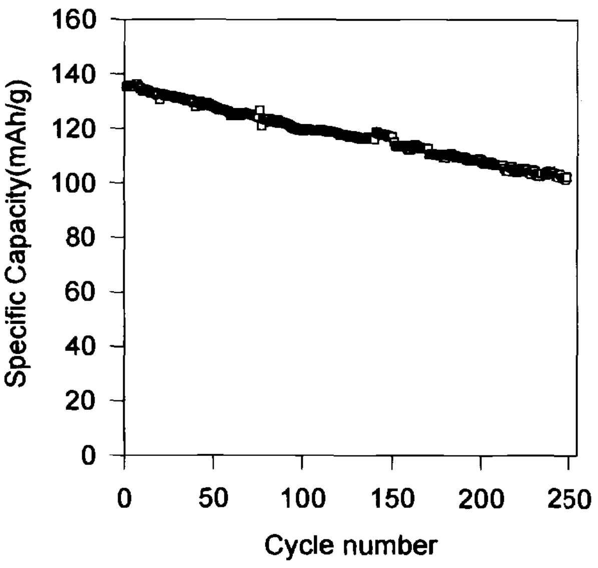

Fig. 10. Discharge capacities of the Li/solid polymer electrolyte/ $Li_{1.03}Mn_2O_4$ cell as a function of cycle number of 0.1 mA/cm^2 (0.2 C rate).

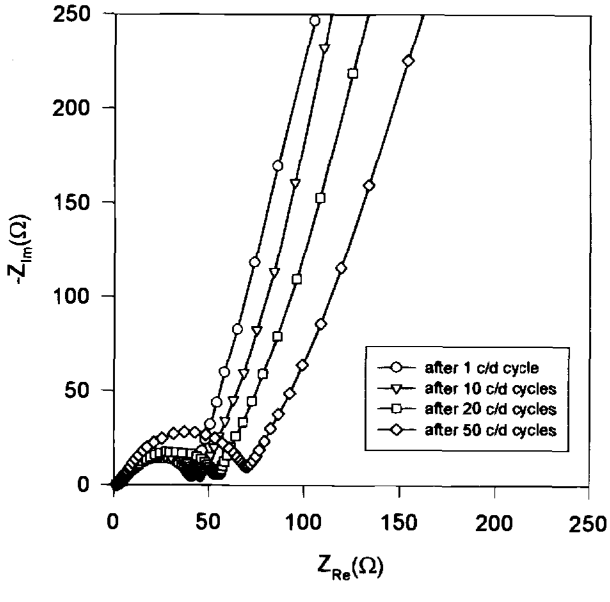

Fig. 11. AC impedance spectra of Li/solid polymer electrolyte/ $Li_{1.03}Mn_2O_4$ cell with the repeated charge/discharge cycles.

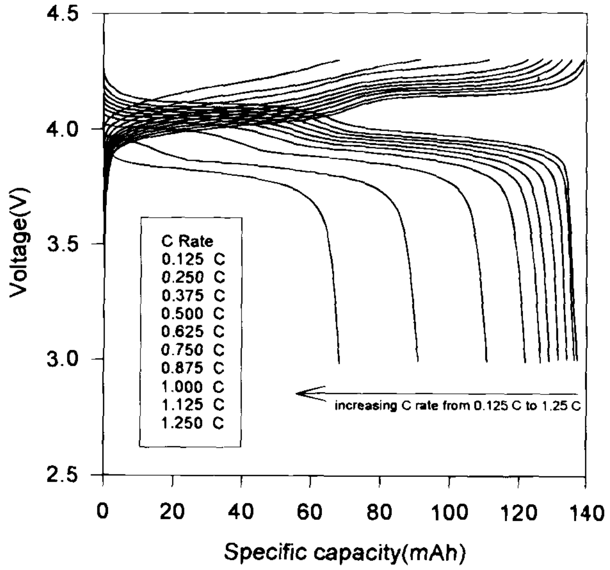

Fig. 12. Charge/discharge curves of Li/solid polymer electrolyte/ $Li_{1.03}Mn_2O_4$ cell at various charge/discharge rates.

Conclusions

The electrochemical properties of the plasticized polymer electrolytes composed of acrylonitrile-methyl methacrylate-styrene terpolymer, liquid electrolyte, and inorganic filler were investigated. The polymer electrolyte systems studied in this work showed high ionic conductivity and acceptable mechanical stability to allow operation in rechargeable lithium batteries. The excellent electrochemical properties enabling the use of these polymer electrolytes in rechargeable lithium polymer batteries have been confirmed by the charge/discharge cycling of Li/polymer electrolyte/$Li_{1.03}Mn_2O_4$ cells.

Manuscript submitted October 9, 1997; revised manuscript received January 21, 1998. This is in part Paper 199 presented at The Electrochemical Society and International Society of Electrochemistry Joint Meeting, Paris, France, August 31-September 5, 1997.

Samsung Advanced Institute of Technology assisted in meeting the publication costs of this article.

REFERENCES

1. M. Watanabe, M. Kanba, K. Nagaoka, and I. Shinohara, *J. Polym. Sci., Polym. Phys. Ed.*, **21**, 939 (1983).
2. F. Croce, F. Gerace, G. Dautzemberg, S. Passerini, G. B. Appetecchi, and B. Scrosati, *Electrochim. Acta*, **39**, 2187 (1994).
3. D. Peramunage, D. M. Pasquariello, and K. M. Abraham, *J. Electrochem. Soc.*, **142**, 1789 (1995).
4. K. Tsunemi, H. Ohno, and E. Tsuchida, *Electrochim. Acta*, **28**, 591 (1983).
5. K. Tsunemi, H. Ohno, and E. Tsuchida, *Electrochim. Acta*, **28**, 833 (1983).
6. M. Alamgir and K. M. Abraham, *J. Electrochem. Soc.*, **140**, L96 (1993).
7. S. Passerini, J. M. Rosolen, and B. Scrosati, *J. Power Sources*, **45**, 333 (1993).
8. H. Hong, C. Liquan, H. Xuejie, and X. Rongjian, *Electrochim. Acta*, **37**, 1617 (1992).
9. D. W. Kim, Y. R. Kim, J. K. Park, and S. I. Moon, *Solid State Ionics*, **106**, 329 (1998).
10. D. W. Kim, Y. R. Kim, Y. K. Sun, B. K. Oh, B. S. Jin, and S. I. Moon, *Polymer (Korea)*, **21**, 861 (1997).
11. Y. K. Sun, *Solid State Ionics*, **100**, 115 (1997).
12. J. M. G. Cowie, in *Polymer Electrolytes. Reviews*, Vol. 1, J. R. MacCallum and C. A. Vincent, Editors, p. 92, Elsevier Applied Science, London (1987).
13. J. E. Weston and B. C. J. Steele, *Solid State Ionics*, **7**, 75 (1982).
14. J. Fan and P. S. Fedkiw, *J. Electrochem. Soc.*, **144**, 399 (1997).
15. J. G. Thevenin and R. H. Muller, *J. Electrochem. Soc.*, **134**, 273 (1987).
16. S. Morzilli, F. Bonini, and B. Scrosati, *Electrochim. Acta*, **32**, 961 (1987).
17. D. Aurbach, I. Weissman, A. Zaban, and O. Chusid, *Electrochim. Acta*, **39**, 51 (1994).
18. W. Liu, G. C. Farrington, F. Chaput, and B. Dunn, *J. Electrochem. Soc.*, **143**, 879 (1996).
19. M. M. Thackery, W. I. F. David, P. G. Bruce, and J. B. Goodenough, *Mater. Res. Bull.*, **18**, 461 (1983).
20. R. Koksbang, I. I. Olsen, P. E. Tonder, N. Kundsen, and D. Fauteux, *J. Appl. Electrochem.*, **21**, 301 (1991).
21. Y. Xia, H. Takeshige, H. Noguchi, and M. Yoshio, *J. Power Sources*, **56**, 61 (1995).
22. P. G. Dickens and G. F. Reynolds, *Solid State Ionics*, **5**, 53 (1981).